EARTH'S CRYOSPHERE
SCIENTIFIC JOURNAL

Earth's Cryosphere, 2024, vol. XXVIII, No. 1, pp. 43–52

GASES AND GAS HYDRATES IN THE EARTH'S CRYOSPHERE

POCKMARKS AND METHANE CONTENT IN LAKE SEDIMENTS OF THE YAMAL PENINSULA

G.E. Oblogov[1,*], A.A. Vasiliev[1], P.T. Orekhov[1,2], A.S. Savvichev[3], I.D. Streletskaya[4]

[1] *Institute of the Earth's Cryosphere, Tyumen Scientific Center, Siberian Branch of the Russian Academy of Sciences, Malygina St. 86, Tyumen, 625000 Russia*
[2] *Arctic Research Station of the Institute of Plant and Animal Ecology, Ural Branch of the Russian Academy of Sciences, Zelenaya Gorka St. 21, Labytnangi, 629400 Russia*
[3] *Winogradsky Institute of Microbiology, Federal Research Center of Biotechnology, Russian Academy of Sciences, Leninsky pr. 33, build. 2, Moscow, 119071 Russia*
[4] *Lomonosov Moscow State University, Leninskie Gory 1, Moscow, 119991 Russia*

*****Corresponding author; e-mail: oblogov@mail.ru*

The paper presents the results of studying the appearance and sizes of pockmarks in lakes of three bioclimatic zones of Yamal: northern (arctic), typical, and southern tundra. The diameter of pockmarks in the lakes increases from 1.9 m in the northern tundra to 7.7 m in the southern shrub tundra. Pockmarks occupy from 0.5 to 4.3% of the shallow-water lake area. The content of methane in lake sediments is two or more times higher than in the sediments of the active and transient layers of dominant landscapes. In the typical tundra zone, the methane content in lake sediments is usually about 7 mL/kg, but in some cases it can reach 18 mL/kg and more. Probably, the lakes with the high methane content in bottom sediments are the lakes, where gas emissions can occur and pockmarks can form. After drainage (drying) of the lakes, lake basins (khasyreys) are subjected to freezing, and the cryogenic structure of lake sediments is formed. Eight–ten years after drying, succession changes in the former lake bottoms continue, and the formation of the transient layer is not yet completed.

Keywords: *permafrost, pockmarks, lakes, Yamal, methane content in sediments.*

Recommended citation: Oblogov G.E., Vasiliev A.A., Orekhov P.T., Savvichev A.S., Streletskaya I.D., 2024. Pockmarks and methane content in lake sediments of the Yamal Peninsula. *Earth's Cryosphere* XXVIII (1), 43–52.

INTRODUCTION

In recent decades, the problem of methane (CH_4) emissions due to climate warming has been actively studied [*AMAP, 2015; Dean et al., 2018; IPCC, 2018*]. Methane is an active greenhouse gas with high global warming potential [*IPCC, 2018*]. Emissions from the surface in the typical and southern tundra of the Arctic and Subarctic can be a serious source of methane entering the atmosphere. From 8 to 29 Tg [CH_4] per year are released into the atmosphere from the surface of Arctic ecosystems annually [*McGuire et al., 2012; Chen et al., 2015*], which accounts for approximately 10% of global methane emissions from natural wetlands [*Ciais et al., 2013; Saunois et al., 2020*].

Methane produced in frozen and thawing sediments of the permafrost zone and emitted into the atmosphere has a predominantly biogenic genesis [*Kraev et al., 2017; Streletskaya et al., 2018*].

Methane entry into the atmosphere is regulated by methane fluxes in the sediment mass below the surface [*Dean et al., 2018*]. It follows that the emission of methane into the atmosphere directly depends on its content in the active layer (AL) and the upper horizons of permafrost. Our studies of the methane content and emissions in the dominant landscapes of the typical and southern tundra have confirmed that methane emissions are completely controlled by the landscape structure. High emissions are inherent in the landscapes of swamps (including floodplains), surface water runoff hollows, and drained lake basins (khasyreys); the highest content of CH_4 is observed in the AL and upper permafrost in the same landscapes [*Zadorozhnaya et al., 2022*]. With an increase in air temperature, the metabolism of microorganisms of near-surface sediments, including methanogens, should increase. On the example of the western coast of Yamal, an increase in the methane content in the AL with the rise in the AL temperature has indeed been established [*Vasiliev et al., 2022*].

The contribution of lakes to the total flux of methane into the atmosphere is estimated in different ways. O.A. Anisimov believes that methane transport in the form of bubbles from the bottoms of the lakes, especially in the coastal shallow part of them, is a powerful source of methane emission [*Anisimov et al., 2020*]. However, direct observations of CH_4 emis-

Fig. 1. A gas pockmark in the sediments of a drained lake.

The Erkuta site, southern Yamal. Photo by P.T. Orekhov.

sions from the lake water indicate that methane fluxes are insignificant [*Glagolev et al., 2011; Sabrekov et al., 2011*]. At the same time, observations of methane fluxes from lakes by the method of isolated chambers are carried out in conditions, when there are no bubble methane fluxes from the bottom of the lake. This is due to the fact that methane bubble emissions occur impulsively over a short period of time. It is not even clear yet whether the areas of methane bubble emissions are permanent, or whether they form each time in a different place. According to A. Portnov's indirect data, the "lifetime" of bubble fluxes in the southern part of the Kara Sea is hours to first days [*Portnov et al., 2013*]. Bubble emissions create specific landforms on the seabed in the form of predominantly rounded funnels with a diameter from 10–20 m to 600 and even 1000 m, sometimes forming into groups [*Judd, Hovland, 2007*]. In studies of methane emissions from the bottom of the Arctic seas, such crater-like depressions are called pockmarks. Obviously, this term can also be applied to funnels at the bottom of the lakes (Fig. 1), since they are formed by similar mechanisms of the upward migration of fluids (i.e., gas or liquid) as a result of the release of accumulated gas. In both cases, both in seeps from pockmarks in the seas and in seeps from lake sediments, methane has mainly biogenic genesis [*Judd, Hovland, 2007; Kallistova et al., 2019; Savvichev et al., 2023*].

Similar in origin and morphology are the unique phenomena of terrestrial permafrost – gas emission funnels – that have been comprehensively studied after the discovery of the Yamal funnel to the south of the Bovanenkovo oil and gas condensate field in July 2014 [*Leibman, Plekhanov, 2014; Kizyakov et al., 2015; Bogoyavlensky et al., 2017*]. Their formation is associated with the occurrence of frozen sediments (and/or massive ice beds) from the surface, which prevent the relatively free release of the accumulated volume of gas in the near-surface sediments. Unlike the gas emission funnels on land, gas accumulation in lake sediments occurs in thawed unlithified rocks, and a large amount of gas is not required for gas escape under high pressure.

During the evolution of permafrost landscape under the impact of climate changes and neotectonic and cryogenic processes, lakes are sometimes drained and khasyreys are formed. After that, vegetation settles on drained bottoms of former lakes and the freezing of lake sediments begins. This leads to the transformation of microrelief, the development of various cryogenic processes, and the formation of new landscape features. Studies of the long-term dynamics of lakes in the permafrost zone under conditions of climate warming [*Jones et al., 2022*] indicate that in the continuous permafrost subzone, the number of drained lakes is approximately the same as the number of lakes increasing in their area. In the subzone of discontinuous permafrost, the area of lakes tends to decrease, and the area of drained lake basins with mire vegetation increases [*Webb, Liljedahl, 2023*]. The drainage of lakes may be due to a faster formation of large taliks with climate warming [*Farquharson et al., 2022*].

The process of formation of underwater gas funnels (pockmarks) in lakes, their distribution in various bioclimatic zones, and their morphology have not been studied at all, but have been recorded by many researchers [*Kuzin, 1992; Sizov, 2015; Bogoyavlensky et al., 2016*]. There are virtually no data on the methane content in lake sediments at the bottom of lakes and after their drainage and transformation into khasyreys [*Dvornikov et al., 2019*]. In this regard, the aim of our work was to study the likely patterns of the development of lake pockmarks and their sizes and to assess the methane content in the sediments of lake basins and khasyreys in the bioclimatic zones of the northern (Arctic), typical and southern tundra of the Yamal Peninsula.

STUDY AREA

The study of the distribution and morphology of pockmarks in lakes was carried out at three sites (Fig. 2) in different bioclimatic zones of Yamal: the northern (subzone C according to [*Walker et al., 2009*]), typical (subzone D), and southern (subzone E) tundra. Lakes in the northwestern part of Bely Island were studied in the northern tundra subzone, a site near the Marre-Sale Weather Station was represented the typical tundra, and lakes in the Erkuta Station area were studied in the southern tundra.

The research site on Bely Island is located on the surface of the first marine terrace at 8–12 m a.s.l. in the vicinity of the M.V. Popov Weather Station. The

vegetation cover is typical of the northern tundra and is represented by thin lichens and mosses with sedges in waterlogged areas. The surface is almost flat and slightly dissected. Lakes occupy about 15% of the territory. Marine sediments are represented by saline fine-grained sands with syngenetic polygonal ice wedges. The territory of Bely Island is in the area of continuous permafrost. Within the first marine terrace, the mean annual permafrost temperature was –9.5°C in 1972 and increased to –8.6°C in 1978 and –7.1°C in 2009. Within coastal meadows affected by tides (laydas), the mean annual permafrost temperature is 1.0–1.5°C higher [*Vasil'chuk, Vasil'chuk, 2015*]. Usually, the mean annual temperature in lake basins is higher than on the main surface by 1.0–1.5°C due to the increased accumulation of snow [*Vasiliev et al., 2020*]. The average depth of seasonal thawing of sandy soil at the CALM R55A site in 2022 was 123 cm; seasonal thawing of swampy loamy sandy soil at site R55 averaged 54 cm.

In western Yamal, the research was carried out in the area of Marre-Sale Weather Station on the marine terrace elevated at 20–29 m a.s.l. The vegetation cover is represented by mosses, lichens, forbs and sedges; there are also dwarf shrubs (cloudberry, blueberry and lingonberry) and willow shrubs. The surface of the terrace is dissected by ravines, hollows, and nested lake basins. The lake area is about 12% of the territory [*Zadorozhnaya et al., 2022*]. There are two units in the geological structure of the third marine terrace. The upper unit is represented by lacustrine–alluvial and eolian nonsaline sands and loamy sands on the Holocene (MIS 1) and Sartan (MIS 2) ages. These sediments contain syngenetic ice wedges. They are underlain by sandy, loamy sandy, and loamy coastal and marine sediments of the Karginskii (MIS 3) age. The base of the section is composed of the Kazantsevskii (MIS 5) saline marine clays and loams. It is often impossible to separate the Kazantsevskii and Karginskii sediments, so they are sometimes combined into the Marresal formation [*Gataullin, 1991*]. Sediments of MIS 3 and MIS 5 contain massive ice beds. The area belongs to the continuous permafrost subzone with a thickness of about 90 m; below, there are cryotic rocks, whose thickness has not been determined. The mean annual permafrost temperature in watersheds in this area increased from –6.5°C in 1979 to –5.0°C in 2000 and –4.0°C in 2022. In lake basins, the mean annual permafrost temperature 1.5–1.8°C higher [*Vasiliev et al., 2020*]. The average depth of seasonal thawing on sandy surfaces at CALM R3 site in 2022 was about 180 cm; on a swampy surface, 59 cm.

In southern Yamal, the study of pockmarks was carried out in the area of the Erkuta Station of the Institute of Plant and Animal Ecology of the Ural Branch of the Russian Academy of Sciences, on the surface of the second marine terrace elevated at about 15–20 m a.s.l. The vegetation cover is typical for the

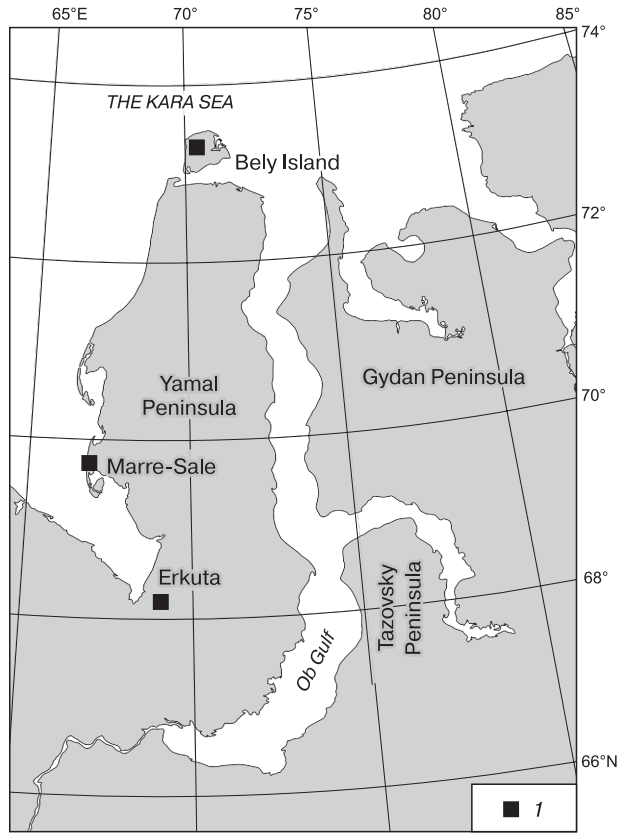

Fig. 2. A schematic map of the key sites' location.

1 – study areas.

southern shrub tundra and is represented by herb–moss–lichen associations. Willow shrubs reach a height of 1.0–1.5 m. The surface of the marine terrace is flat, slightly dissected. Lakes cover about 20% of the area. The Quaternary sediments of the marine terrace are represented almost exclusively by fine-grained nonsaline sands. The area belongs to the continuous permafrost subzone, though relatively deep closed taliks are formed on floodplains. The mean annual permafrost temperature on watersheds in this area was measured only in 1979 and was about –5.5°C [*Chuvilin et al., 2020*]. By analogy with the rate of temperature rise on Bely Island and in the Mare-Sale area, the current mean annual permafrost temperature in the Erkuta area is expected to be about –2.5 to –3.5°C. In the lake basins, the mean annual permafrost temperature is about 1.5°C higher. The average depth of seasonal thawing on the moistened sandy surface at CALM R58 site in 2022 was 101 cm.

Thus, the study areas cover the bioclimatic zones of the northern, typical, and southern shrub tundra. Lake area percentage varies from 12% at the Marre-Sale site to more than 20% at the Erkuta site. Geocryologically, all observation sites are located in the area of continuous permafrost with the range of mean

annual temperatures from –7.0 to –2.5°C. It should be noted that, according to the observations of A.V. Pavlov in the Marre-Sale area [*Pavlov, 2008*], the mean annual temperature of sediments at the bottom of shallow (<1 m) lakes is 6 to 8°C higher than the mean annual air temperature and reaches 0 to +3.7°C. Under all of the studied lakes, there are closed taliks. At all the sites, surface permafrost layers are ice rich and contain ice wedges; in the sections of Quaternary sediments at the Erkuta and Marre-Sale sites, massive ice beds are also present.

RESEARCH METHODOLOGY

The study of underwater pockmarks in lakes is based on their identification from satellite and aerial photographs from unmanned aerial vehicles (UAVs), statistical analysis of their size, shape, and spatial distribution. The primary identification of the pockmarks was carried out through a visual search for promising lakes in the Yandex.Maps online service [*http://yandex.ru/maps*] based on satellite images from WorldView-2, IKONOS, Landsat-7, Sentinel, SPOT-1-5 and others. Lakes with an extensive shallow part were identified, in which the presence of pockmarks was assumed. In the selected key areas, an UAV survey was carried out in the field. In the area of Bely Island, the survey was carried out using the Geoscan 201 Geodesy complex (produced by Geoscan, Russia) from a height of 500 m. In other areas, a DL Mavic 2 Pro shooting quadcopter (Dajiang Innovation Technology Co., China) was used. In the Marre-Sale area, the survey was carried out from a height of 500 m; in the Erkuta area, 330 m.

The spatial resolution of the UAV cameras made it possible to identify objects of up to 0.5 m in size. The resulting images were geometrically corrected and converted into a UTM cartographic projection (WGS-84) in the ArcGIS software package (ESRI, USA). For a more detailed visual definition of the pockmarks, color-gamma correction of the images was performed. The edges of lakes, areas of underwater elevations to depths of about 2 m, and all possible areas of pockmarks were identified. Based on the obtained area data, the main statistical indicators of the size, distribution areas, and the character of the pockmark size distribution were calculated. The size of the pockmarks was calculated on the basis of data on their area with the assumption of their perfectly circular shape. To estimate the spatial distribution of pockmarks within the lake areas under consideration, the tool of the ArcGIS package "average nearest neighbor" was used. This tool made it possible to measure the distance between the centers of neighboring pockmarks and average these distances. If the average distance turned out to be less than the average for a hypothetical random distribution (the Nearest Neighbor Ratio (NNR) is less than 1), such a distribution of objects was considered clustered (objects are grouped into local groups); if NNR is more than 1, the distribution was considered random or uniform.

The methane content in the sediments of the lake basins was determined in detail in the area of the typical Marre-Sale tundra. Samples of the most undisturbed structure were selected from the rocks of the seasonal thawing layer and the upper horizon of permafrost. The sampling was carried out manually using a 76-mm diameter core sampler. Soil samples in khasyreys were taken with a cutting ring from the walls of seven pits excavated to the permafrost table and somewhat deeper, or to the maximum possible depth within the AL. The samples were manually adjusted to a cylindrical shape with a volume of about 50 cm^3, weighed with an accuracy of 0.01 g, and placed into plastic syringes Jane with a volume of 150 mL. At each sampling point, the features of the microrelief, vegetation, water conditions at the surface, and lithological composition of the soil samples were described. The total moisture content of the sediments was determined every 10 cm according to a standard method. Degassing of the samples was carried out in the field using the HeadSpace method [*Alperin, Reeburgh, 1985; Kampbell et al., 1989*]. Gas samples from the gas-air mixture in syringes (with a volume of about 50 mL) were pumped into 10-mL glass vials and then transported to the laboratory. The methane concentration was analyzed by gas chromatography at the S.N. Vinogradsky Institute of Microbiology of the Russian Academy of Sciences (Moscow) on a Crystal-2000M flame ionization detector (Chromatek production, Russia). The accuracy of determining the methane concentration was ±5% of the measured value.

CHANGES IN CLIMATIC CONDITIONS OF THE YAMAL PENINSULA

The northern part of Yamal belongs to the territory with the Arctic marine climate; the central part of the peninsula is characterized by the Subarctic marine climate, and the southern part has a moderately continental climate. In accordance with the latitudinal zoning on the peninsula, mean annual air temperatures increase from north to south. Other climatic characteristics also change. For estimates of methane content and emissions, the air temperature and the duration of the warm period, during which methane production occurs, are important. Climate warming in Yamal has been observed since the 1970s and proceeds with an average rate of 0.05°C/yr. The analysis of spatial changes demonstrated that, in the period from 1970 to 2020, the isolines of the mean annual air temperature shifted northeast by about 80–100 km [*Malkova et al., 2018*].

Table 1 presents data on the mean annual air temperature and the duration of the warm period for the period of the climatic norm (1961–1990) and for the relatively cold 2021 and warm 2022 for three

Table 1. **Climatic characteristics of key sites**

Weather station	Mean annual oil temperature, °C			Duration of the worm period, days		
	1961–1990	2021	2022	1961–1990	2021	2022
Bely Island	–11.2	–8.8	–5.9	111	120	128
Marre-Sale	–8.4	–7.1	–4.0	120	131	137
Erkuta	–6.6	–5.6	–2.9	128	136	140

Yamal weather stations. In the areas of Bely Island and Marre Sale, the work was carried out in the immediate vicinity of weather stations, and the climatic characteristics for Erkuta were taken according to the weather station Salekhard, located about 100 km south of the observation site.

As follows from Table 1, there is a steady increase in the mean annual air temperatures in the direction from north to south. According to the climatic norm, the difference between mean annual air temperatures on Bely Island and in Salekhard is 4.6°C; in 2021, it was 3.2°C; in 2022, 3.0°C. According to Table 1, it is possible to assume a decrease in the rate of the mean annual air temperature rise with climate warming. However, a more detailed analysis of climate data is needed to confirm this phenomenon.

With climate warming from 1970 to 2020, the duration of the warm season on the Bely Island and in the Marre-Sale area increased by 17 days; in the Salekhard region, by 12 days. The increase in the duration of the warm season is mainly due to the later transition to subzero daily temperatures in the fall.

RESULTS AND DISCUSSION

Size distribution of pockmarks

At each observation site, one lake with the largest number of pockmarks was selected from the UAV images. Coordinates of the selected lakes are as follows: Bely Island 73°19′ N, 70°16′ E; Marre-Sale 69°42′ N, 66°51′ E; Erkuta 68°11′ N, 68°43′ E. Figure 3 presents fragments of UAV images of the studied lakes with pockmarks. Pockmarks are mainly found in the shallow zone of lakes. It is possible that they may be present in deeper parts of the lakes, but the applied research method does not allow them to be traced due to the opacity of a thicker water layer. Although, it can be noted that the prevailing opinion is about the presence of pockmarks only in the shallow part of the lakes [*Anisimov et al., 2020*].

The area of the pockmarks and their diameters were measured at the three sites. On Bely Island, 101 pockmarks were identified; in Marre-Sale, 150; in Erkuta, 94. Statistical indicators of the area and size of pockmarks are presented in Table 2.

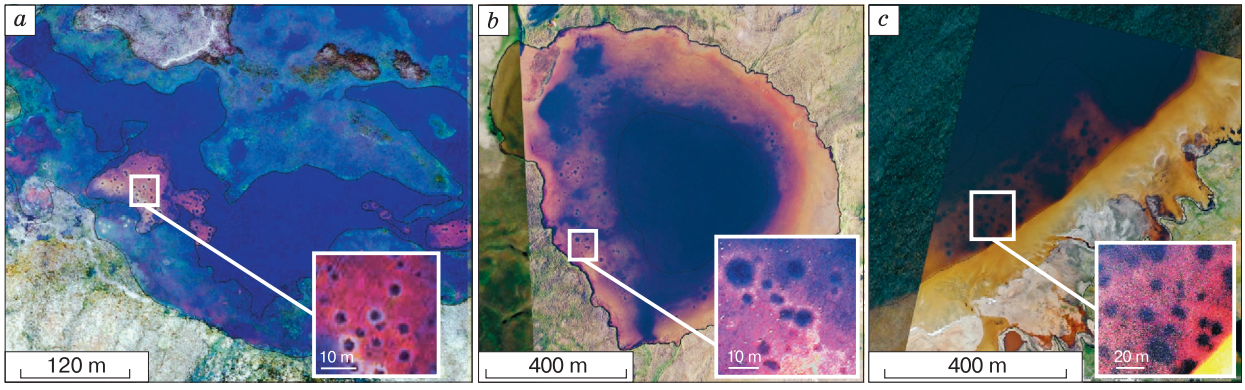

Fig. 3. UAV images of the lake (part of the lake) with pockmarks and enlarged fragments with corrected color-contrast images in the regions of:

a – Bely Island, *b* – Marre-Sale observation site, and *c* – Erkuta observation site. The rectangle highlights the area of the snapshot fragment.

Table 2. **Statistical indicators of pockmarks in lakes of the key sites**

Weather station	Pockmark area, m^2					Pockmark diameter, m				
	min	max	mean	median	st. dev.	min	max	mean	median	st. dev.
Bely Island	0.5	23.9	3.4	2.6	3.0	0.8	5.5	1.9	1.8	0.8
Marre-Sale	1.6	77.2	15.4	10.8	13.4	1.4	9.9	4.1	3.7	1.7
Erkuta	5.2	117.7	50.7	45.6	27.1	2.6	12.2	7.7	7.6	2.2

A sufficient number of measurements of the pockmark sizes allowed us to construct size distribution curves of the pockmarks (Fig. 4).

It can be seen from Table 2 and Figure 4 that the sizes of pockmarks in different bioclimatic zones differ markedly from each other. In the northern (Arctic) tundra, pockmarks with a diameter of about 1.5 m prevail, their occurrence is about 50%; pockmarks with a diameter of more than 4 m are not found. The average diameter of the pockmarks in this region is (1.9 ± 0.8) m. In the typical tundra (Marre-Sale), the highest occurrence is typical for pockmarks of about 4 m in diameter (40%). The average diameter of the pockmarks increases to (4.1 ± 1.7) m. The largest pockmarks were found in the area of the Erkuta site, where the predominant diameter of the pockmarks is about 8 m (35.5%). The average diameter of the pockmarks reaches (7.7 ± 2.2) m. Thus, the results of studying the size of gas pockmarks give grounds to assert that as the transition from the northern tundra to the southern shrub tundra is accompanied by a fourfold increase in the average diameter of the pockmarks (from 1.9 to 7.7 m). This is probably related to a higher productivity of methanogenesis in conditions of higher temperatures of lake sediments. In addition, it is known that as the temperature of the environment increases, the species composition of methanogenic archaea with accelerated metabolism changes [*McCalley et al., 2014*].

All discovered gas pockmarks are confined to the shallow part of the lakes. The spatial distribution of gas pockmarks in the studied key areas of the lakes turned out to be different. The NNR coefficient for the considered part of the lake in the area of Bely Island is 1.07. The average distance between two neighboring pockmarks is about 5 m. In the Marre-Sale area, the NNR coefficient is 0.66, which indicates the unification of pockmarks into separate local groups. At the same time, the average distance between two adjacent pockmarks is about 19 m. In the Erkuta area, in the considered part of the lake, the NNR coefficient is 1.24, which indicates a random distribution. The average distance between two adjacent pockmarks here is about 21 m.

The total area of the pockmarks in relation to the total area of the shallow part of the lakes was 4% on Bely Island, 0.5% in the Marre-Sale area, and 4.3% in the Erkuta area.

Methane in lake sediments

There are little data on the methane content in sediments of lake taliks. The study of methane content in the silty sediments of lakes in Central Yamal was conducted by a group of researchers led by M.O. Leibman and A.Y. Khomutov [*Savvichev et al., 2021*]. They took samples of bottom mud from four lakes and determined the methane content in semiliquid bottom sediments. The density of bottom sediments varied from 1100 kg/m^3 in the near-surface part to 1300 kg/m^3 in the deeper horizons. The testing was carried out to a depth of up to 15 cm from the bottom. The results were presented in tabular form. Based on these data, the distribution of methane content by depth in bottom sediments was constructed. Since the data for the three lakes turned out to be very close, they were combined into one group. The methane content in the fourth lake was very different from the first group, so they are shown separately (Fig. 5).

An exponential function was used as an approximation-model for the first group, and for Lake 003 (the numbering of lakes is given according to [*Savvichev et al., 2021*]) drawing an approximation line does not make sense, since there are only three points here.

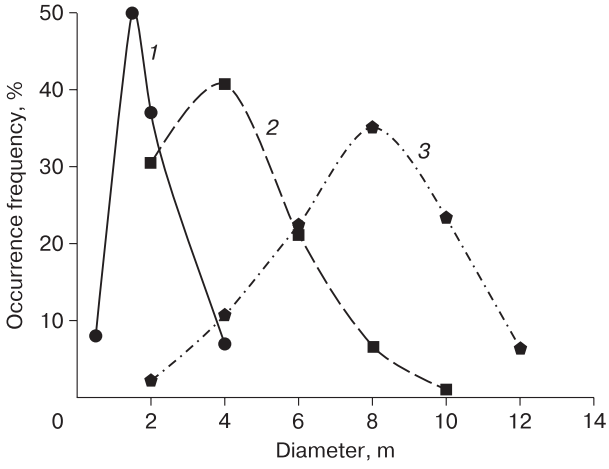

Fig. 4. Distribution curves of diameters of pockmarks in lakes of the key sites.

1 – Bely Island, *2* – Marre-Sale, *3* – Erkuta.

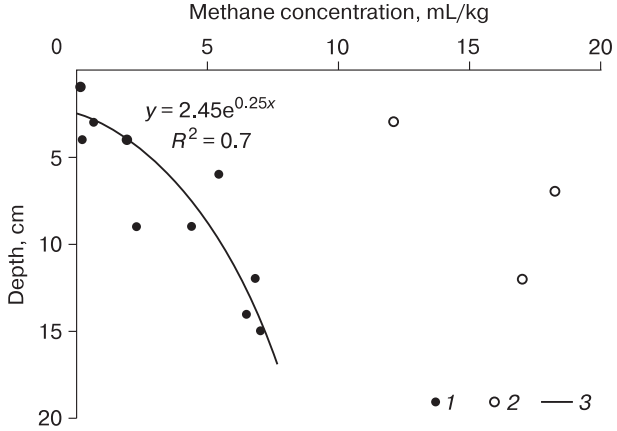

Fig. 5. Distribution of methane concentrations by depth in bottom sediments of the lakes in Central Yamal (according to [*Savvichev et al., 2021*]).

1 – lakes 010, 002, 004; *2* – lake 003; *3* – approximation curve by exponential function.

As can be seen from Fig. 5, in the first group of lakes, the distribution of methane concentration by depth is characteristic of the diffusion mechanism of methane transport from deeper horizons to the surface of the lake bottom. Near the surface, the concentration of methane is close to zero; at a depth of about 15 cm, it reaches 7 mL/kg. The methane concentration in the bottom sediments of Lake 003 is much higher and reaches 18.3 mL/kg. The methane content in the bottom sediments of lakes both in the first group and especially in Lake 003 significantly exceeds the background methane content in sediments of the seasonally thawed and transient layers in all types of dominant landscapes of the typical tundra. The methane content does not exceed 4.5 mL/kg in the typical tundra, and its usual values are 2–4 mL/kg [*Zadorozhnaya et al., 2022*]. The average concentration of methane in lake sediments in the Bykovsky Peninsula (northern Yakutia) reaches 25 mL/kg [*Yang et al., 2023*]. Probably, the high methane content in Lake 003 and in the lakes of Bykovsky Peninsula indicate the possibility of bubble mechanism of methane transport from depth to the surface of the bottom of lakes and the formation of pockmarks. In any case, it can be stated that the concentration of methane in lake sediments is significantly higher compared to that in sediments of the AL in all dominant landscapes. This is due to a higher level of metabolism and methane production by anaerobic archaea at elevated ambient temperatures.

The study of methane content in sediments of the drained lake basin (khasyrey) was carried out in the Marre-Sale area. Here, a small lake with a diameter of about 200 m (69°41′ N, 66°48′ E) and a depth of no more than 2 m, located near the shore of the Kara Sea on the surface of the third marine terrace was drained due to the advance of a ravine developing along polygonal wedged ice from the shore to the lake. In 2012, the boundary of the ravine reached the lake, and in 2012–2013 the lake descended. The drained basin immediately began to be developed by pioneer vegetation, and by 2021 plant associations corresponding to the local soil moistening conditions were formed (Fig. 6).

Fig. 6. Vegetation at the bottom of the lake drained in 2013 as of 2021.

Marre-Sale area. Photo by K.A. Nikitin.

The microrelief of the former lake bottom is still incompletely shaped; there are well-drained elevated areas and, on the contrary, overmoistened and paludified depressions. Small water pools are preserved, and no traces of gas pockmarks have been found in them. In more drained areas, moss–herb cover is formed; waterlogged areas are occupied by moss–cotton grass associations. The sediments composing the lake depression are represented by fine-grained sands and loamy sands. Actually, lake sediments with a thickness of less than 1 m differ from the indigenous coastal-marine sands in a finer texture (silty loamy sands) and a darker brow color due to the high content of organic matter. The underlying sands have a yellowish gray color. The boundary between them is quite distinct.

In August 2021, a profile across the former lake bottom was laid; eight soil pits along the profile were excavated to the AL depth and, in some cases, penetrated into the upper permafrost horizon. The results of determining the methane content in the khasyrey sediments are presented in Fig. 7. This figure also shows data on the methane content in a separate (69°42′ N, 66°49′ E) lake depression in waterlogged (20MS11) and drained (21MS5) areas.

As seen from Fig. 7, data on methane concentrations can be divided into two groups. The first group includes soils with low concentrations (0.005–

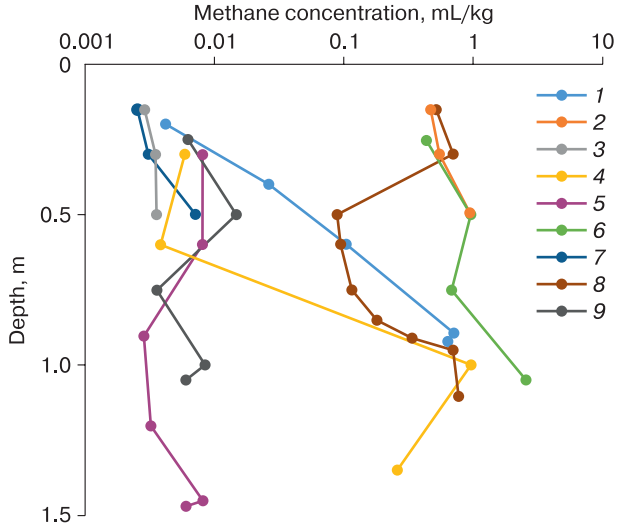

Fig. 7. Methane concentration in lacustrine sediments, Marre-Sale area.

Pit numbers: *1* – 21MS13, *2* – 21MS14, *3* – 21MS15, *4* – 21MS16, *5* – 21MS17, *6* – 21MS18, *7* – 21MS19, *8* – 20MS11, *9* – 21MS5.

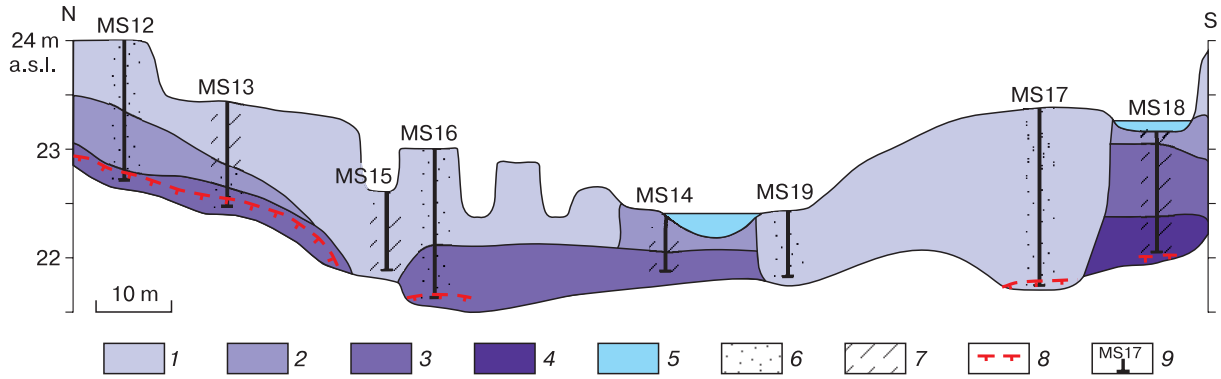

Fig. 8. Schematic cross-section of the spatial distribution of methane in the khasyrey sediments in the Marre-Sale area.

1–4: methane content in the rock, mL/kg: *1* – 0 to 0.1, *2* – 0.1 to 0.5, *3* – 0.5 to 1, *4* – >1; *5* – water; *6*, *7*: lithological composition of sediments: *6* – sand, *7* – loamy sand; *8* – lower boundary of the seasonally thawed layer; *9* – location and number of the pit.

0.03 mL/kg) of methane (left part of the graph) typical of drained sands on elevated elements of local topography. Methane concentrations are exceptionally low and do not differ from methane concentrations in drained sandy landscapes beyond the lake basin [*Zadorozhnaya et al., 2022*]. In inundated and waterlogged areas, the methane concentration is significantly higher and reaches 1 mL/kg (right part of the graph) and even 2.5 mL/kg (one sample). In both cases, the methane content roughly corresponds to its content in similar landscapes of the main surface and is controlled mainly by moistening conditions.

A detailed study of the methane content in the AL and the underlying frozen sediments on the studied profile makes it possible to estimate the spatial distribution of the methane content in the lake sediments of the khasyrey (Fig. 8). In Fig. 8, an uneven scale of methane concentrations is selected for the best illustration.

The formation of the final landscape appearance of the khasyrey has not yet been completed, the relief is being smoothed, the hydrological regime is being rebuilt, and the surface is being developed by various plant associations. Therefore, it can be assumed that the distribution of methane in the section has not yet been fully formed. The layered structure of methane distribution is well expressed in the marginal parts of the khasyrey, which is characterized by a low methane content in the near-surface layers of sediments. The methane content increases with depth. The lower frozen horizon at the foot of the AL with the highest methane content of up to 2.5 mL/kg can be interpreted as a transient layer according to [*French, Shur, 2010*], in which the methane content is 2–5 times higher than in the upper horizons.

In the central part of the khasyrey, a layered distribution of methane is observed only under the residual lake; in other parts of the center of the khasyrey, there is no layered distribution. It can be assumed that over the past 8–10 years after the lake was drained, the transient layer has not yet fully developed.

CONCLUSIONS

The studies carried out on Bely Island, in the Marre Sale area, and at the Erkuta stationary observation site allow us to draw some conclusions about the patterns of pockmark development and methane content in lacustrine sediments of Yamal.

The manifestation and size of pockmarks in lakes of three bioclimatic zones of Yamal – northern, typical, and southern tundra – have been studied. Average diameter of pockmarks naturally increase from 1.9 m in the northern tundra to 7.7 m in the southern shrub tundra following an increase in air temperature. The authors attribute this to the intensified methane production due to the accelerated metabolism of methanogenic archaea at higher temperatures of lacustrine deposits in the south of the studied region compared with the north.

All pockmarks are confined to the shallow part of the lakes. The distribution of pockmarks over the area of lakes is different: in the lake near Marre-Sale, they form local clusters; in lakes on Bely Island and at the Erkuta site, their distribution is irregular.

Pockmarks occupy from 0.5% to 4.3% of the shallow water area of the lakes.

The methane content in lacustrine deposits is two or more times higher than that in sediments of the STL and transient permafrost layer in dominant landscapes of typical tundra. This confirms the higher level of methanogenesis in lakes compared to land. Most likely, in lakes with a very high methane content in lake sediments, a bubble mechanism of methane transport and emission with the formation of pockmarks can be realized.

The methane content in the changing landscape conditions of the newly formed and freezing khasyreys is characterized by strong variability. Using the example of the Marre-Sale area, it was found that over 8–10 years after the lake drainage, successional changes in vegetation and the formation of the transient layer continue.

Acknowledgments. *The authors are grateful to the reviewers and editors of the journal for their work to improve the quality of the paper.*

This study was carried out within the framework of state assignment of the Institute of the Earth's Cryosphere no. FWRZ-2021-0005 "Patterns of Formation and Degradation of Subaqueous and Coastal Marine Permafrost in the Seas of the Western Sector of the Russian Arctic" and with the support of the Scientific Center for Arctic Studies (Salekhard).

References

Alperin M.J., Reeburgh W.S., 1985. Inhibition experiments on anaerobic methane oxidation. *Appl. Environ. Microbiol.* **50** (4), 940–945. DOI: 10.1128/AEM.50.4.940-945.1985

AMAP, 2015. AMAP Assessment 2015: Methane as an Arctic climate forcer. Arctic Monitoring and Assessment Programme (AMAP), Oslo, Norway, 139 p.

Anisimov O.A., Zimov S.A., Volodin E.M., 2020. Methane emission in the permafrost zone of Russia and assessment of its impact on the global climate. *Meteorolog. Gidrolog.* 5, 131–143. (in Russian)

Bogoyavlensky V.I., Bogoyavlensky I.V., Nikonov R.A. et al., 2016. Remote detection of areas of surface gas manifestations and gas emissions in the Arctic: the Yamal Peninsula. *Arktika: Ekolog. Ekonomika* 3 (23), 4–15. (in Russian)

Bogoyavlensky V.I., Bogoyavlensky I.V., Nikonov R.A., 2017. Results of aerospace and expeditionary studies of large gas emissions on Yamal near the Bovanenkovo field. *Arktika: Ekolog. Ekonomika* 3 (27), 4–17. DOI: 10.25283/2223-4594-2017-3-4-17

Chen X., Bohn T.J., Lettenmaier D.P., 2015. Model estimates of climate controls on pan-Arctic wetland methane emissions. *Biogeosciences* **12**, 6259–6277. DOI: 10.5194/bg-12-6259-2015

Chuvilin E., Stanilovskaya J., Titovsky A. et al., 2020. A gas-emission crater in the Erkuta River Valley, Yamal Peninsula: characteristics and potential formation model. *Geosciences* **10** (5), 170. DOI: 10.3390/geosciences10050170

Ciais P., Sabine C., Bala G. et al., 2013. Carbon and Other Biogeochemical Cycles. In: *Climate Change: The Physical Science Basis. Contribution of Working Group I to the Fifth Assessment Report of the Intergovernmental Panel on Climate Change* / Stocker T.F., Qin D., Plattner G.-K. et al. (Eds.). Cambridge, Cambridge Univ. Press, p. 465–570.

Dean J.F., Middelburg J.J., Röckmann T. et al., 2018. Methane feedbacks to the global climate system in a warmer world. *Reviews Geophysics* **56** (1), 207–250. DOI: 10.1002/2017RG000559

Dvornikov Y.A., Leibman M.O., Khomutov A.V. et al., 2019. Gas-emission craters of the Yamal and Gydan peninsulas: A proposed mechanism for lake genesis and development of permafrost landscapes. *Permafr. Periglac. Process.* **30** (3), 146–162. DOI: 10.1002/ppp.2014

Farquharson L.M., Romanovsky V.E., Kholodov A. et al., 2022. Sub-aerial talik formation observed across the discontinuous permafrost zone of Alaska. *Nature Geosci.* **15**, 475–481. DOI: 10.1038/s41561-022-00952-z

French H., Shur Y., 2010. The principles of cryostratigraphy. *Earth-Sci. Rev.* **101** (3–4), 190–206. DOI: 10.1016/j.earscirev.2010.04.002

Gataullin V.N., 1991. Marre-Sale Formation of the Western Yamal: Sediments of the Pra-Ob Delta. *Byull. Kom. Izuchen. Chetvertichn. Perioda* **60**, 53–61. (in Russian)

Glagolev M., Kleptsova I., Filippov I. et al., 2011. Regional methane emission from West Siberia mire landscapes. *Environ. Res. Lett.* **6**, 045214. DOI: 10.1088/1748-9326/6/4/045214

IPCC, 2018. Global Warming of 1.5°C. An IPCC Special Report on the impacts of global warming of 1.5°C above pre-industrial levels and related global greenhouse gas emission pathways, in the context of strengthening the global response to the threat of climate change, sustainable development, and efforts to eradicate poverty / Masson-Delmotte V., P. Zhai H.-O. Pörtner et al. (Eds.). Cambridge Univ. Press, Cambridge, UK and New York, NY, USA, 616 p. DOI: 10.1017/9781009157940

Jones B.M., Grosse G., Farquharson L.M. et al., 2022. Lake and drained lake basin systems in lowland permafrost regions. *Nature Rev. Earth & Environ.* 3, 85–98. DOI: 10.1038/s43017-021-00238-9

Judd A., Hovland M., 2007. Seabed fluid flow around the world. In: *Seabed Fluid Flow: The Impact on Geology, Biology and the Marine Environment*. Cambridge, Cambridge Univ. Press, p. 45–133. DOI: 10.1017/CBO9780511535918.005

Kallistova A.Yu., Savvichev A.S., Rusanov I.I. et al., 2019. Thermokarst lakes, ecosystems with intense microbial processes of the methane cycle. *Microbiology* **88** (6), 649–661. DOI: 10.1134/S0026261719060171

Kampbell D.H., Wilson J.T., Vandegrift S.A., 1989. Dissolved oxygen and methane in water by a GC Headspace Equilibration Technique. *Int. J. Environ. Analytic. Chemistry* **36** (4), 249–257. DOI: 10.1080/03067318908026878

Kizyakov A.I., Sonyushkin A.V., Leibman M.O., 2015. Geomorphological conditions of the gas-emission crater and its dynamics in Central Yamal. *Earth's Cryosphere* XIX (2), 13–22.

Kraev G., Schulze E., Yurova A. et al., 2017. Cryogenic displacement and accumulation of biogenic methane in frozen soils. *Atmosphere* **8** (6), 105. DOI: 10.3390/atmos8060105

Kuzin I.L., 1992. On the nature of anomalous lakes – indicators of hydrocarbon accumulations in the deep horizons of the sedimentary cover. In: *Problems of Assessing New Zones of Oil and Gas Accumulation in the Main Productive Strata of Western Siberia*. St. Petersburg, VNIGRI, p. 129–137. (in Russian)

Leibman M.O., Plekhanov A.V., 2014. Yamal gas outlet funnel: results of a preliminary survey. *Kholod'OK* **2** (12), 9–15. (in Russian)

Malkova G.V., Korostelev Yu.V., Sadurtdinov M.R. et al., 2018. Modern climatic changes and temperature regime of permafrost in the European North. In: *Pressing Problems of Geocryology. Reports of the Extended Meeting of the Scientific Council on Earth Cryology of the Russian Academy of Sciences (Moscow, Moscow State University, May 15–16, 2018)*. Moscow, Univ. Kniga, vol. 1, p. 98–104. (in Russian)

McCalley C., Woodcroft B., Hodgkins S. et al., 2014. Methane dynamics regulated by microbial community response to permafrost thaw. *Nature* 514 (7523), 478–481. DOI: 10.1038/nature13798

McGuire A.D., Christensen T.R., Hayes D. et al., 2012. An assessment of the carbon balance of Arctic tundra: comparisons among observations, process models, and atmospheric inversions. *Biogeosciences* **9** (8), 3185–3204. DOI: 10.5194/bg-9-3185-2012

Pavlov A.V., 2008. *Monitoring of the Cryolithozone*. Novosibirsk, Acad. Publ. House "Geo", 229 p. (in Russian)

Portnov A., Smith A.J., Mienert J. et al., 2013. Offshore permafrost decay and massive seabed methane escape in water depths >20 m at the South Kara Sea shelf. *Geophys. Res. Lett.* **40** (15), 3962–3967. DOI: 10.1002/grl.50735

Sabrekov A.F., Glagolev M.V., Kleptsova I.E., 2011. Contribution of permafrost mounds to methane emission from tundra mires in Western Siberia. *Dinamika okruzh. sredy global'n. izmenen. klimata* **2** (4), 1–11. (in Russian)

Saunois M., Stavert A.R., Poulteret B. et al., 2020. The global methane budget 2000–2017. *Earth Syst. Sci. Data* **12** (3), 1561–1623. DOI: 10.5194/essd-12-1561-2020

Savvichev A., Rusanov I., Dvornikov Yu. et al., 2021. The water column of the Yamal tundra lakes as a microbial filter preventing methane emission. *Biogeosciences* **18** (9), 2791–2807. DOI: 10.5194/bg-18-2791-2021

Savvichev A.S., Rusanov I.I., Kadnikov V.V. et al., 2023. Biogeochemical activity of methane-related microbial communities in bottom sediments of cold seeps of the Laptev Sea. *Microorganisms* **11** (2), 250. DOI: 10.3390/microorganisms11020250

Sizov O.S., 2015. Remote analysis of the consequences of surface gas shows in the north of Western Siberia. *Geomatika* 1, 53–68. (in Russian)

Streletskaya I.D., Vasiliev A.A., Oblogov G.E. et al., 2018. Methane content in ground ice and sediments of the Kara Sea coast. *Geosciences* **8** (12), 434. DOI: 10.3390/geosciences8120434

Vasil'chuk A.C., Vasil'chuk Yu.K., 2015. Engineering-geological and geochemical conditions of polygonal landscapes of Bely Island (Kara Sea). *Inzhenern. Geologiya* 1, 50–65. (in Russian)

Vasiliev A.A., Drozdov D.S., Gravis A.G. et al., 2020. Permafrost degradation in the Western Russian Arctic. *Environ. Res. Lett.* **15** (4), 045001. DOI: 10.1088/1748-9326/ab6f12

Vasiliev A.A., Melnikov V.P., Zadorozhnaya N.A., 2022. Methane content and emission in the typical tundra and the southern tundra of the Western Russian Arctic. *Dokl. Earth Sci.* **505** (1), 506–511. DOI: 10.1134/S1028334X22070170

Walker D.A., Raynolds M.K., Daniëls F.J.A. et al., 2009. The Circumpolar Arctic Vegetation Map. *J. Veget. Sci.* **16** (3), 267–282. DOI: 10.1111/j.1654-1103.2005.tb02365.x

Webb E.E., Liljedahl A.K., 2023. Diminishing lake area across the northern permafrost zone. *Nature Geosci.* **16**, 202–209. DOI: 10.1038/s41561-023-01128-z

Yang S., Anthony S.E., Jenrich M. et al., 2023. Microbial methane cycling in sediments of Arctic thermokarst lagoons. *Glob. Change Biol.* **29** (10), 2714–2731. DOI: 10.1111/gcb.16649

Zadorozhnaya N.A., Oblogov G.E., Vasiliev A.A., 2022. Methane in frozen and thawing sediments of Western Russian Arctic. *Earth's Cryosphere* XXVI (5), 35–47.

URL: http://yandex.ru/maps (last visited: 01.05.2023).

Received March 28, 2023
Revised May 31, 2023
Accepted December 7, 2023

Translated by S.B. Sokolov